UHASSELT
KNOWLEDGE IN ACTION

Maastricht University

Faculty of Medicine and Life Sciences
School for Life Sciences
Master of Biomedical Sciences

Master's thesis

PDE4D enzymes as a possible therapeutic target to alleviate memory loss in Alzheimer's disease

Jule Richartz

Thesis presented in fulfillment of the requirements for the degree of Master of Biomedical Sciences, specialization Molecular Mechanisms in Health and Disease

SUPERVISOR :

Prof. dr. Tim VANMIERLO

MENTOR :

Mevrouw Emily WILLEMS

2023
2024

Transnational University Limburg is a unique collaboration of two universities in two countries: the University of Hasselt and Maastricht University.

UHASSELT
KNOWLEDGE IN ACTION

www.uhasselt.be
Universiteit Hasselt
Campus Hasselt:
Martelarenlaan 42 | 3500 Hasselt
Campus Diepenbeek:
Agoralaan Gebouw D | 3590 Diepenbeek

Faculty of Medicine and Life Sciences
School for Life Sciences
Master of Biomedical Sciences

Master's thesis

PDE4D enzymes as a possible therapeutic target to alleviate memory loss in Alzheimer's disease

Jule Richartz

Thesis presented in fulfillment of the requirements for the degree of Master of Biomedical Sciences, specialization Molecular Mechanisms in Health and Disease

SUPERVISOR :

Prof. dr. Tim VANMIERLO

MENTOR :

Mevrouw Emily WILLEMS

PDE4D enzymes as a possible therapeutic target to alleviate memory loss in Alzheimer's disease*

Jule Richartz[1], Emily Willems[1,2] and Tim Vanmierlo[1,2]

[1]Department of Neuroscience, Biomedical Research Institute, Universiteit Hasselt, Campus Diepenbeek, Agoralaan Gebouw C - B-3590 Diepenbeek, Belgium
[2]Department of Psychiatry & Neuropsychology, School for Mental Health and Neuroscience, Maastricht University, 6229 ER Maastricht, The Netherlands

*Running title: *A protocol optimization for PDE4D isoform ablation*

To whom correspondence should be addressed: Prof. Dr. Tim Vanmierlo, Tel: +32 (11) 26 92 28; Email: tim.vanmierlo@uhasselt.be

Keywords: Alzheimer's disease, PDE4D, CRISPR/Cas9, SH-SY5Y, magnetofection.

ABSTRACT

About 50 million people worldwide suffer from Alzheimer's disease, which is the primary cause of all dementia cases. Currently, effective treatment strategies are lacking. The cAMP-PKA-CREB pathway is essential for synaptic plasticity and memory formation. cAMP can be enzymatically degraded by the phosphodiesterase (PDE) enzyme family. Research shows that inhibition of the PDE4 enzyme family by Roflumilast improves memory performance in humans and rodents, but causes side effects. As PDE4D is identified as the predominant subtype involved in cognitive function, selective targeting of PDE4D on the isoform level (PDE4D1-9) could enhance memory consolidation without evoking side effects. This study aims to optimize the transfection protocol of the designed CRISPR/Cas9 sgRNAs for each specific PDE4D isoform in a human neuroblastoma cell line (SH-SY5Y cells), to eventually unravel the role of each isoform in neurite elongation and memory consolidation. Therefore, sgRNAs were designed, developed, and evaluated in a cell-free cleavage assay and gel electrophoresis. The PDE4D isoform expression of SH-SY5Y cells was checked by qPCR, with/without Aβ exposure. Notably, the isoforms PDE4D1 and -7 were not expressed in this cell line after 48h of cell culture. Finally, the transfection protocol was optimized, with 1,75µL of magnetic beads, 500ng of plasmid DNA of PDE4Dpan, and 30min on the magnet resulting in the highest Cas9/DAPI area (30%). The puromycin administration to select the transfected cells still needs to be optimized, as 1µg/mL is lethal for the transfected cells. In conclusion, this transfection protocol can be utilized for further experiments regarding memory consolidation in AD.

INTRODUCTION

One of the most common neurodegenerative disorders worldwide is known as Alzheimer's disease (AD). This disease is age-related as it affects 50% of individuals above 85 years old (1). Nowadays, more than 50 million people worldwide suffer from AD, which is mainly expressed in progressive memory loss and cognitive decline (2, 3). AD is responsible for 60-70% of all dementia cases and is primarily distinguished from moderate cognitive impairment by the loss of independence, which has a major functional impact on the daily life of the patients, but also on their surroundings (4). The presence of amyloid-beta (Aβ) plaques and neurofibrillary tangles (NFT) are the main pathological features of this disease. Aβ plaques are created when amyloid precursor protein (APP) is sequentially cleaved by γ-secretase and beta-site amyloid precursor protein cleaving enzyme 1 (BACE1) (5). These Aβ proteins can accumulate and cause synapse damage but also induce deficits in cognition and electrophysiology (5). Aside from the Aβ plaques, hyperphosphorylated tau will aggregate and form NFT, inducing neurotoxicity (6). Both pathological processes will cause neurodegeneration with loss of synapses and neurons, resulting in cognitive problems and macroscopic atrophy (7).

The primary symptom of AD is memory loss, defined as a progressive and irreversible

cognitive impairment affecting different areas of the brain, like the hippocampal and temporal regions (7, 8). Psychotropic medications such as N-methyl-D-aspartate (NMDA) receptor antagonists (e.g. memantine) and cholinesterase inhibitors (ChE-Is; e.g. donepezil, galantamine, rivastigmine) are frequently recommended and licensed for the treatment of AD. However, not all patients (20-40%) respond positively to these medications and they experience several adverse effects, such as headaches and constipation for memantine, and gastrointestinal, cardiac, and genitourinary symptoms for ChE-Is (9, 10). In addition, these current therapies for AD memory loss slow down but do not stop deterioration or manage cognition (7, 11). For this reason, it is crucial to comprehend the molecular processes and mechanisms involved in memory consolidation, as pathways in this process are often impeded in memory loss. One of the main downstream cascades includes an important second messenger, called cyclic adenosine monophosphate (cAMP). cAMP can allosterically activate cAMP-dependent protein kinase A (PKA), which will phosphorylate the cAMP response binding protein (CREB). This cAMP-PKA-CREB pathway is important in long-term memory formation, ultimately executing its function through activating CREB, initiating the transcription and translation of crucial genes necessary during synaptic plasticity and memory formation (12-14). Moreover, phosphorylated CREB initiates the expression of brain-derived neurotrophic factor (BDNF), an essential neurotrophic factor in the protection of neurodegeneration (15). Previous research indicated that activation of CREB promotes neurogenesis, while inactivation of CREB promotes Aβ-induced synapse loss, confirming the importance of CREB in memory (16, 17). Moreover, it was discovered that there is a decreased CREB-mediated gene expression in the brains of AD mouse models and patients, as well as in Aβ-damaged cultured neurons (13). In addition, a rise in cytoplasmic cAMP has been shown to improve neuronal synaptogenesis, memory, and mitochondrial biogenesis, and decrease tau-phosphorylating and CREB-inhibiting kinases (18). An explicit example of the latter are GPR40 receptor (polyunsaturated fat receptors) agonists, which can increase the content of cAMP and thus upregulate downstream neurotrophic factors important in neuroprotection (19).

cAMP can be enzymatically degraded by the phosphodiesterase (PDE) enzyme family (14). Their function is to hydrolyze cyclic nucleotides, such as cAMP, highlighting the importance of this enzyme family in the pathway of memory consolidation. There are 11 enzymes identified, of which the cAMP-specific phosphodiesterase 4 (PDE4) enzyme is predominantly present in the brain. The PDE4 family consists of four subtypes, namely PDE4A, -B, -C, and -D. Further, each PDE4 subtype can be divided into long, short, and super-short isoforms, which lead to a difference in regulation (20). Research in 2016 showed that inhibition of the PDE4 enzymes can improve memory consolidation in rodents by using the PDE4 inhibitor Roflumilast (21). Unfortunately, this application is impeded by different severe side effects, such as nausea and vomiting (22). Side effects could be omitted by using a more subtype-selective enzyme approach. Accordingly, the subtype PDE4D appears to be particularly important in cognitive functions. Although there are PDE4D inhibitors (e.g. Gebr32a, HT-0712, BPN14770) that improve cognitive function *in vivo* and are currently in clinical interventions, deletion of PDE4D in mice reduced α2 adrenoreceptor mediated anesthesia that is associated with the side effect of emesis (23). Therefore, a more selective targeting approach of the different protein isoforms of the PDE4D gene could enhance memory consolidation without evoking side effects (24). Since there are no specific inhibitors for the protein isoforms of PDE4D, Paes *et. al.* managed to eliminate the different protein isoforms by CRISPR/Cas9 in an HT22 mouse hippocampal cell line, discovering the effect of the long isoforms on the improvement of neurite elongation, possibly contributing to a positive effect on neuroplasticity and memory formation (25). Moreover, in human AD brain samples, the PDE4D isoforms 1, 3, 5, and 8 are upregulated in expression and show changes in DNA methylation or hydroxymethylation in their promotor region, highlighting the importance of this isoform-selective targeting (12).

Although Paes *et. al.* discovered positive results regarding the targeting of the PDE4D isoforms and their effect on neuroplasticity in mice models, it is still crucial to translate these results into the human context, as the PDE4

biology of mice and humans are similar yet different. The structural variations in the genetic regions of each variant and the number of amino acids ensure that there is a need for validation of the already obtained results in mouse models, this time in human models (26). By examining the human environment, this research aims to provide more insights into the role performed by the various PDE4D isoforms in AD, potentially elucidating a specific PDE4D target to alleviate memory loss. As previously mentioned, there are no inhibitors for the specific PDE4D isoforms, which is why this study will focus on utilizing CRISPR/Cas9 as a knockout tool to ablate these isoforms.

This research aims to design sgRNAs to separately knockout human PDE4D isoforms by CRISPR/Cas9 and create a successful method to study the effects of the different PDE4D isoforms in human neurons *in vitro*. This investigation will provide information about the effectiveness of the transfection of the sgRNAs to human neurons, ultimately providing the foundation for further research to investigate the most potent targets for memory loss in AD. We expect that this research will yield an effective method by utilizing CRISPR/Cas9 and magnetofection for the investigation of the effects of different PDE4D isoforms in a humanized context.

EXPERIMENTAL PROCEDURES

Cell culture – SH-SY5Y human neuroblastoma cells (ATCC, CRL-2266) were cultured in T75 cm^2 culture flasks with DMEM/F-12 supplemented with 10% fetal calf serum (FCS, Biowest), 1% non-essential amino acids (NEAA, Sigma), 2% L-glutamine (L-Glut, Gibco), and 1% penicillin/streptomycin (Pen/Strep, Sigma). Cells were maintained at 37°C with 5% CO_2 and passaged at 80% - 90% confluency. For qPCR and transfection assays, cells were trypsinized (Gibco) and plated in culture medium.

Quantitative PCR – Cells were plated in culture medium at 100.000 cells per well in a 24-well plate. After 48h and 96h, cultures were lysed in Qiazol (Qiagen). For treatment with 1 µM $A\beta_{1-42}$, cells were lysed after 24h of exposure to $A\beta_{1-42}$. RNA was extracted using a standard phenol/chloroform method. RNA quantity and purity were measured using a nanodrop spectrophotometer (Isogen Life Science). Subsequently, cDNA was synthesized by qScript™ cDNA SuperMix (Quanta Biosciences) according to the manufacturer's protocol. All qPCR reactions were performed using 5ng/µL cDNA, 5 µL Fast SYBR-Green Master Mix (Thermo Fisher Scientific), 0.3 µL of both forward and reverse primer (Supplementary Table 2), and the QuantStudio 3 qPCR machine (Applied Biosystems). The Fast reaction protocol consisted of a hold stage (95°C for 20 sec with increasing 4.14°C/sec), the PCR stage (95°C for 1 sec and 60°C for 20 sec with decreasing 3.17°C/sec), and the Melt Curve stage (95°C for 1 sec with increasing 4.14°C/sec, 60°C for 20 sec with decreasing 3.17°C/sec, and 95°C for 1 sec with increasing 0.1°C/sec). Raw Ct values were manually analyzed and relatively expressed by utilizing the start fluorescence values at cycle 0 (Log10 start fluorescence) of the PDE4D isoforms primers. Logarithmic fluorescence values were normalized against the expression of reference genes HMBS and YWHAZ.

CRISPR/Cas9 sgRNA design for PDE4D isoforms – Single guide RNAs (sgRNA) targeted against human PDE4D isoform-specific DNA sequences were designed with the online web tool Benchling.com and were checked for target specificity via BLAST (Supplementary Table 1). In addition, the frameshift frequency was checked by the machine learning algorithm InDelphi. The sgRNAs were ordered by Integrated DNA Technologies (Leuven, Belgium) and annealed using the PCR thermocycler according to the following parameters: 37°C for 30min, followed by 95°C for 5min, and ramp down to 25°C at 0.1°C/sec. Subsequently, they were digested and ligated in a one-step PCR reaction in a pSpCas9(BB)-2A-Puro (PX459, Addgene #62988) vector, using the Bbsl-I enzyme (BioLabs), rCutsmart buffer (BioLabs), T4 DNA ligase (BioLabs), 10X T4 DNA ligase buffer (BioLabs), and autoclaved MilliQ. The vectors including the sgRNAs were transformed by heat-shock into DH5α *E. coli*, cultured in ampicillin-containing Luria-Bertani (LB) agar plates for subsequent colony selection. Single colonies were picked and cultured in LB medium, followed by vector isolation and purification using a NucleoSpin Plasmid DNA Purification kit (Macherey-Nagel), according to the manufacturer's instructions. Validation of sgRNA insertion was performed through Sanger sequencing (Macrogen Europe) by utilization of the PXSeq Forward primer (5'-AGGGCCTATTTCCCATGATT-3'). Vectors

with the correct sgRNAs inserted were expanded and purified by the Invitrogen PureLink™ HiPure Plasmid Maxiprep Kit, according to the manufacturer's instructions. A colony without the sgRNA incorporated in the PX459 vector was utilized as a negative control. The purified vectors were stored at -20°C.

sgRNA in vitro transcription by gel electrophoresis – A cell-free cleavage assay was performed using the Guide-It sgRNA *In Vitro* Transcription and Screening System (Takara Bio) according to the manufacturer's instructions. The primers (Supplementary Table 3) and forward sequences including sgRNA (Supplementary Table 4) were designed for PDE4D3, -5, -9, and -pan. In addition, the DNA of SH-SY5Y cells was isolated by the DNeasy Kit (QIAGEN) and 600-800bp amplicons were generated through the utilization of the primers (Supplementary Table 3) and a polymerase mix. 10µL of the PCR product was added on a 1.5% agarose gel with a 100bp DNA ladder (Invitrogen) to visualize the cleaved and uncleaved products.

Puromycin optimization – SH-SY5Y cells were plated in 24- and 96-well plates (DAPI staining and MTT respectively). After 48h of culture, eight concentrations of puromycin were tested: 0; 0,25; 0,5; 1; 2; 3; 5; and 10 µg/mL. Puromycin (Invivogen) was diluted in supplemented DMEM/F-12. The cells with puromycin were maintained at 37°C with 5% CO_2 for 72h. The mortality of the cells was examined by adding 12.5µL MTT, diluted in 100µL culture medium, for 4h to the wells. After administration of 150µL DMSO and 25µL glycine in each well, the absorbance was measured by the plate-reader (CLARIOstar) at 550nm. In addition, a DAPI staining of 10min was executed to check the mortality of the cells.

Optimization of cell transfection – For the magnetofection optimization, SH-SY5Y cells were plated in 24-well plates at 150.000 cells per well on 12mm glass coverslips (VWR) and cultured for 48h. Next, cells were treated with plasmid DNA and magnetic beads. Two concentrations (500ng vs 1000ng) of the PDE4Dpan plasmid DNA and two concentrations (1.75µL vs 3.5µL) of magnetic beads (NeuroMag, Oz Biosciences) were tested. In addition, two different durations (30min and 4h) of cells on the magnet (Oz Biosciences) were taken into account. For each testing condition (2 wells/condition), one well was treated with Puromycin (1µg/mL) and was administered for 72h after 48h of magnetofection. The other well without puromycin was used for immunocytochemistry. Cells were checked for morphology every 24h either by general light microscopy (Zeiss, 30min magnetofection) or by means of the IncuCyte (Essen Bioscience, 4h magnetofection). transfected for 30min were checked every 24h

Immunocytochemistry staining – Five days after transfection, SH-SY5Y cells were fixated for 20min by 4% paraformaldehyde and blocked with 1% BSA in 0.1% PBS-Tween for 30min. Cells were incubated with mouse anti-Cas9 (1:1000; MAC133, Merck) primary antibody for 4h in blocking buffer. After washing with PBS, cells were incubated with goat anti-mouse Alexa-Fluor 488 (1:600, Invitrogen) secondary antibody in blocking buffer for 1h at 4°C. Finally, cells were counterstained for 10min with DAPI for the nuclei. After mounting the cells on microscope glasses using Fluoromount (Invitrogen), the transfected cells were imaged by the Leica DFC450 C fluorescence microscope. The images were analyzed by the area of Cas9 divided by the area of DAPI, expressed in percentage (%).

Statistical tests – Data was checked for normality by the Shapiro-Wilk test. Outliers were detected by the ROUT test and removed before statistical analysis. To detect the differences in mRNA expression of the PDE4D isoforms with and without $A\beta_{1\text{-}42}$ administration, a two-tailed non-parametric t-test was performed on each PDE4D isoform separately.

RESULTS

SH-SY5Y cells express all the PDE4D isoforms, except for PDE4D7 – To investigate the PDE4D isoform expression profile of the SH-SY5Y cells at two different time points (48h and 96h of culture), a qPCR analysis was performed. Ultimately, the data was compared to the start fluorescence of each PDE4D isoform (Figure 1). After both 48h (Figure 1a) and 96h (Figure 1b) of cell culture, the mRNA of the long isoform PDE4D7 was not expressed. This result will be taken into account according to further experiments targeting the different PDE4D isoforms. Besides PDE4D7, all other mRNAs of the PDE4D isoforms were expressed after 48h and 96h of cell culturing. However, the mRNA of the short isoform PDE4D1 has

only little expression at both time points. In contradiction, the mRNA of the long isoform PDE4D5 is highly expressed in comparison to the start fluorescence of the primers. Regarding the adequate expression pattern of the mRNAs on the PDE4D isoforms after 48h, this time point will be utilized in the transfection protocol.

SH-SY5Y cells with $A\beta_{1-42}$ exposure have a relatively higher trend of PDE4D expression – Since the main goal of this research is to ablate different PDE4D isoforms independently in an AD-like model, the expression pattern of both SH-SY5Y cells with and without $A\beta_{1-42}$ exposure for 24h was established (Figure 2). According to previous data, cells will be maintained in culture for 48h before qPCR

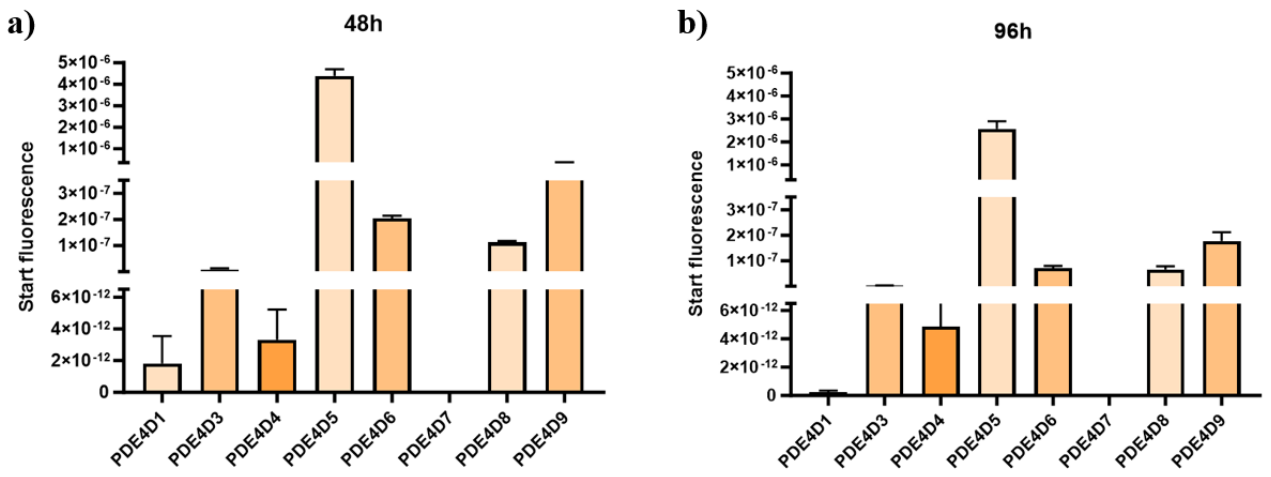

Figure 1 – **PDE4D isoform expression profile of SH-SY5Y cells assessed by qPCR.** The mRNA expression of the different isoforms was measured after 48h **(a)** and 96h **(b)** of cell culture and expressed relative to the start fluorescence of the PDE4D primers. All PDE4D isoform mRNAs were expressed after 48h and 96h of cell culturing, except for PDE4D7. Data are represented as mean ± SEM (n = 3). *PDE; phosphodiesterase, SEM; standard error of mean.*

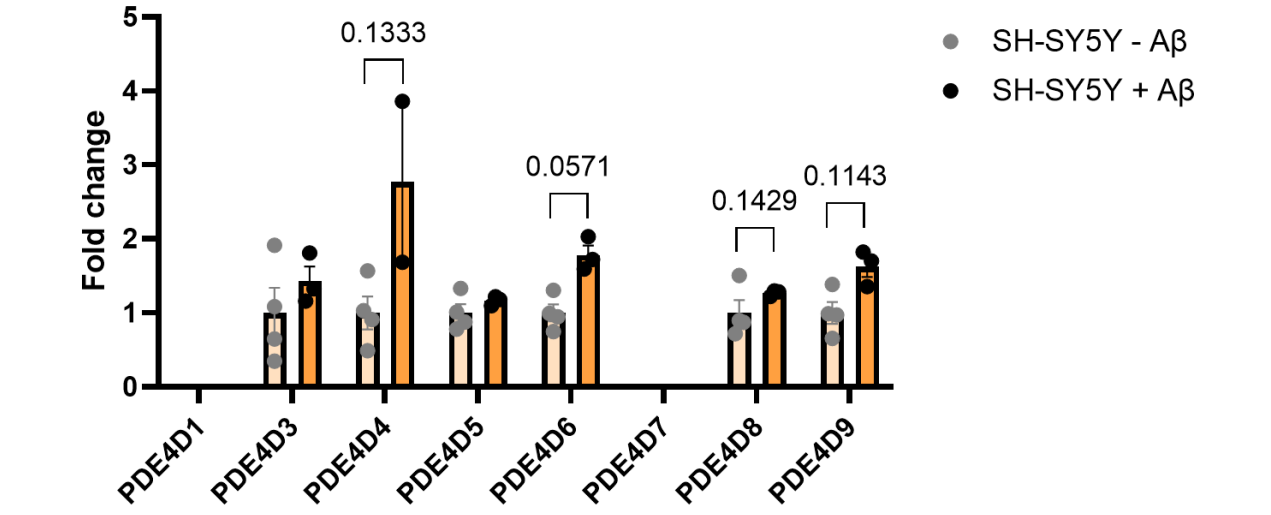

Figure 2 – **The mRNA expression pattern of different PDE4D isoforms in SH-SY5Y with and without $A\beta_{1-42}$ exposure by qPCR.** mRNA expression of SH-SY5Y cells with $A\beta_{1-42}$ exposure (SH-SY5Y + Aβ) is depicted relatively to the mRNA expression of the SH-SY5Y cells without $A\beta_{1-42}$ exposure (SH-SY5Y – Aβ), expressed as fold change. Both mRNAs of PDE4D1 and -7 were not expressed in the SH-SY5Y cells with and without $A\beta_{1-42}$ exposure. Data are represented as mean ± SEM (n = 2-4). The two-tailed non-parametric t-test was performed for each isoform separately, and no significant differences were detected. P-values close to a trend (PDE4D4, -8, -9) and p-values close to a significant difference (PDE4D6) are given in the figure. *PDE; phosphodiesterase, Aβ; Abeta, SEM; standard error of mean.*

analysis (Figure 1). Both mRNAs of the isoforms PDE4D1 and -7 were not expressed in SH-SY5Y cells with or without $A\beta_{1-42}$ exposure, which will be taken into account in further experiments focusing on the transfection with the CRISPR/Cas9 plasmids. The mRNA expressions of the other PDE4D isoforms were not significantly different when $A\beta_{1-42}$ was administered. However, there is a clear trend in the mRNA expression of PDE4D6 of the SH-SY5Y cells without $A\beta_{1-42}$ in comparison to the SH-SY5Y cells with $A\beta_{1-42}$ administration (p-value = 0.0571).

The CRISPR/Cas9 sgRNAs of PDE4D3, -5, -9, and -pan can successfully cleave the DNA sequence of interest – For the different CRISPR/Cas9 plasmids, designed for each specific PDE4D isoform, the capacity of the sgRNAs to cut the DNA sequence of interest was examined. Therefore, an *in vitro* cell-free cleavage assay was performed of four sgRNAs (3, 5, 9, and pan), chosen by the high expression profile after 48h (PDE4D5, -9) (Figure 1a), a sgRNA with more base pairs in comparison to the other PDE4D sgRNAs (PDE4D3) (Supplementary Table 1), and the sgRNA that can fully ablate the PDE4D enzymes (PDE4Dpan). The outcome of the assay was performed by agarose gel electrophoresis, where the bands of the uncleaved amplicons and cleaved amplicons are visible (Figure 3). According to the total amplicon lengths and fragment sizes computed (Supplementary Table 3), all sgRNAs with Cas9 protein have cut between the desired base pairs.

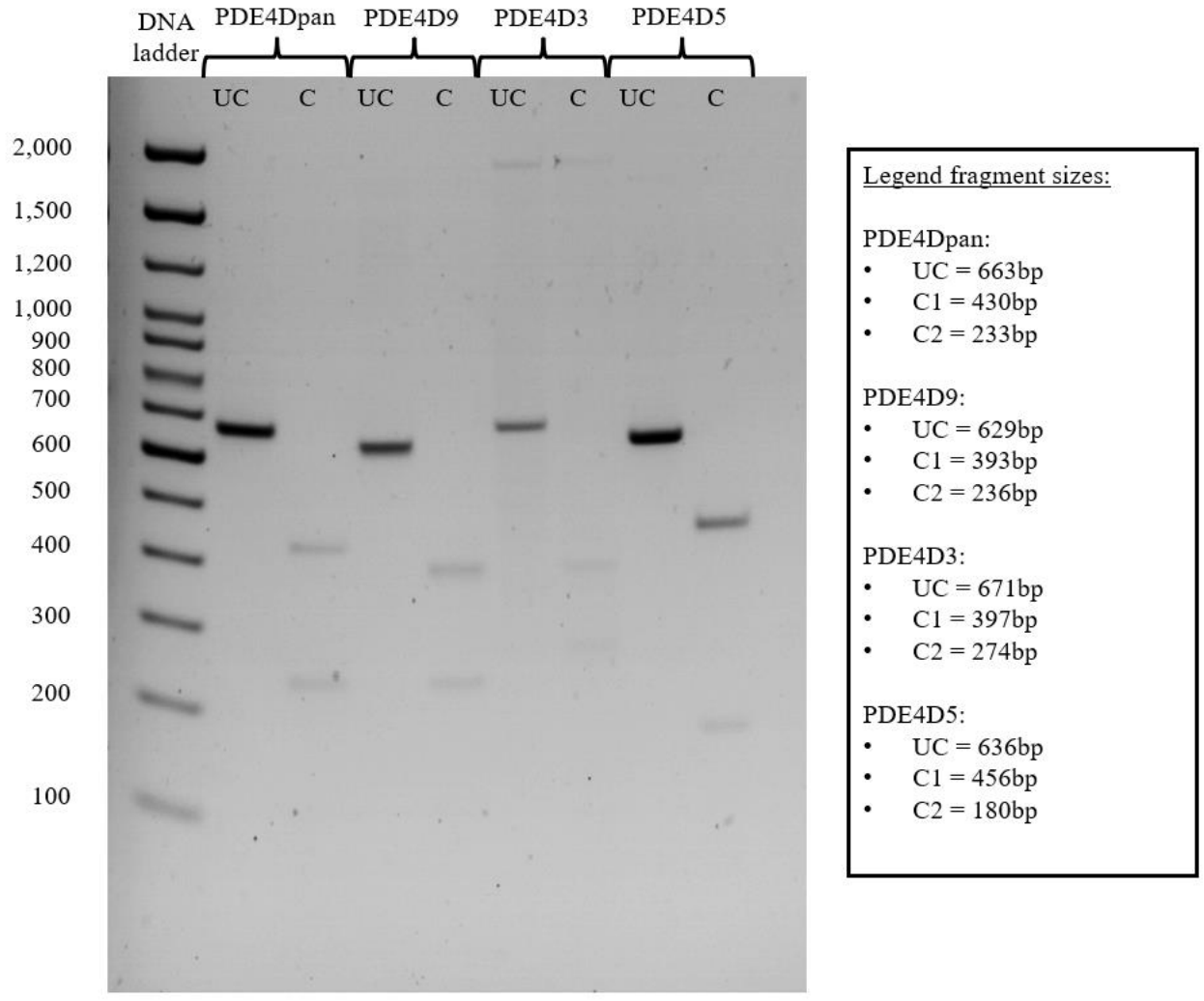

Figure 3 – *In vitro* cleavage assay of sgRNAs of four different PDE4D isoforms (PDE4D3, -5, -9, -pan). Based on the 100bp DNA ladder and Supplementary Table 3, the uncleaved amplicons (UC) are successfully cleaved in the cleaved (C) fragments of the different PDE4D isoform targets. The legend describes the corresponding lengths of the UC amplicon and C fragments. *sgRNA; single guide RNA, PDE; phosphodiesterase, bp; base pair, UC; uncleaved, C1; cleaved fragment 1, C2; cleaved fragment 2.*

The optimal dose of puromycin for SH-SY5Y cell selection after transfection is 1µg/mL – An MTT assay was performed with 8 different concentrations of puromycin to check the lethality of the untransfected SH-SY5Y cells (Figure 4a). 0µg/mL is a negative control for the puromycin lethality, as no puromycin was administered to the cells and all cells were viable, translated in a relative absorbance of 1. With increasing concentrations of puromycin, the relative absorbance decreases gradually. The concentration of 0,5µg/mL still reflects an average relative absorbance of 0,58, while 1µg/mL firmly decreases the relative absorbance to an average of 0,16. Furthermore, the concentrations 2, 3, 5, and 10µg/mL all represent an overkill of the SH-SY5Y cells, with an average relative absorbance of 0,11. To validate these findings, a DAPI staining on the untransfected SH-SY5Y cells with five different puromycin concentrations (0, 1, 3, 5, and 10µg/mL) was performed (Figure 4b). This immunocytochemistry staining confirms the data from the MTT assay, as the SH-SY5Y cells with 0µg/mL puromycin are prominently present and viable by a high amount of DAPI, in contrast to the concentrations 3, 5, and 10µg/mL, where only a few DAPI stainings were imaged (one per image). Here again, the cells with 1µg/mL puromycin administration have a higher amount of DAPI staining in comparison to 3, 5, or 10µg/mL, but still a firmly decreased amount of DAPI in comparison to the negative control (0µg/mL).

Transfection of the PDE4Dpan plasmid in SH-SY5Y cells by magnetofection is successful – To eventually ablate the different PDE4D isoforms in SH-SY5Y cells, the transfection protocol needs to be optimized. Therefore, six different conditions were tested, including differences in the concentration of beads (1,75µL vs 3,5µL), plasmid DNA (500ng vs 1000ng), and time on the magnet (30min vs 4h). Observation of the immunocytochemistry stainings 5d after transfection already verifies the successful transfection of the PDE4Dpan plasmid with Cas9 into the SH-SY5Y cells by the overlaps visible of the Cas9 and DAPI staining (Figure 5a). Besides, as visible on the immunocytochemistry image of 3,5µL magnetic beads and 500ng of plasmid DNA, there are some additional Cas9 spots on the background. After quantification of the immunocytochemistry stainings (Figure 5b), we can validate the transfection as the percentage of the Cas9 area over the DAPI area is higher in

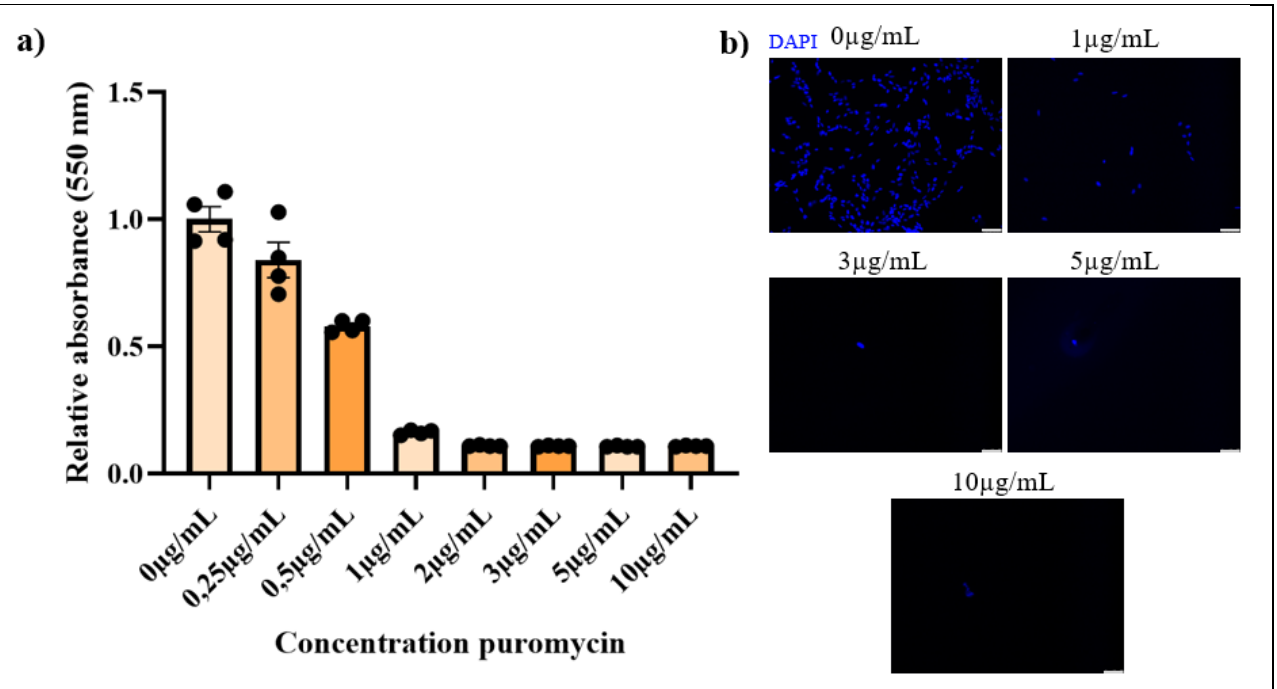

Figure 4 – Optimizing the puromycin concentration for selection of transfected cells. (a) Quantitative analysis of the MTT assay of 8 different concentrations of puromycin on non transfected SH-SY5Y cells, expressed as relative absorbance (normalized to the negative control 0µg/mL). **(b)** Immunocytochemistry staining of 5 conditions puromycin administered to non transfected SH-SY5Y cells. Images represent a DAPI (blue) staining of the nuclei of the living cells. The scale bar represents 50µm (n = 4). *µg; microgram, mL; milliliter, nm; nanometer, DAPI; 4',6-diamidino-2-phenylindole.*

all conditions compared to the non transfected cells, for both 30min and 4h on the magnetic plate. Furthermore, the condition with 1,75µL of magnetic beads, 500ng of DNA, and 30min on the magnet resulted in the highest percentage of Cas9/DAPI area (30,38%), while the other conditions represent approximately 20% of Cas9/DAPI area. Unfortunately, this cannot be validated by statistical tests as there is only a sample size of 1 for each group.

1µg/mL puromycin is lethal for the SH-SY5Y cells after magnetofection – To selectively isolate the cells successfully transfected with the PDE4Dpan plasmids, 1µg/mL puromycin was administered to the cells 48h after magnetofection as optimized in the MTT assay (Figure 4a). Light microscopy images were taken of the conditions with 30min on the magnetic plate, each 48h after magnetofection, and 72h after puromycin administration (5d after magnetofection) (Figure 5c). The images illustrate that after 48h and 5d after magnetofection without puromycin administration, the cells have a normal morphology. When puromycin was added in a concentration of 1µg/mL after 5d of magnetofection, all cells of all conditions died. The same results were seen on the IncuCyte images for the conditions with 4h on the magnetic plate (Supplementary Figure 1).

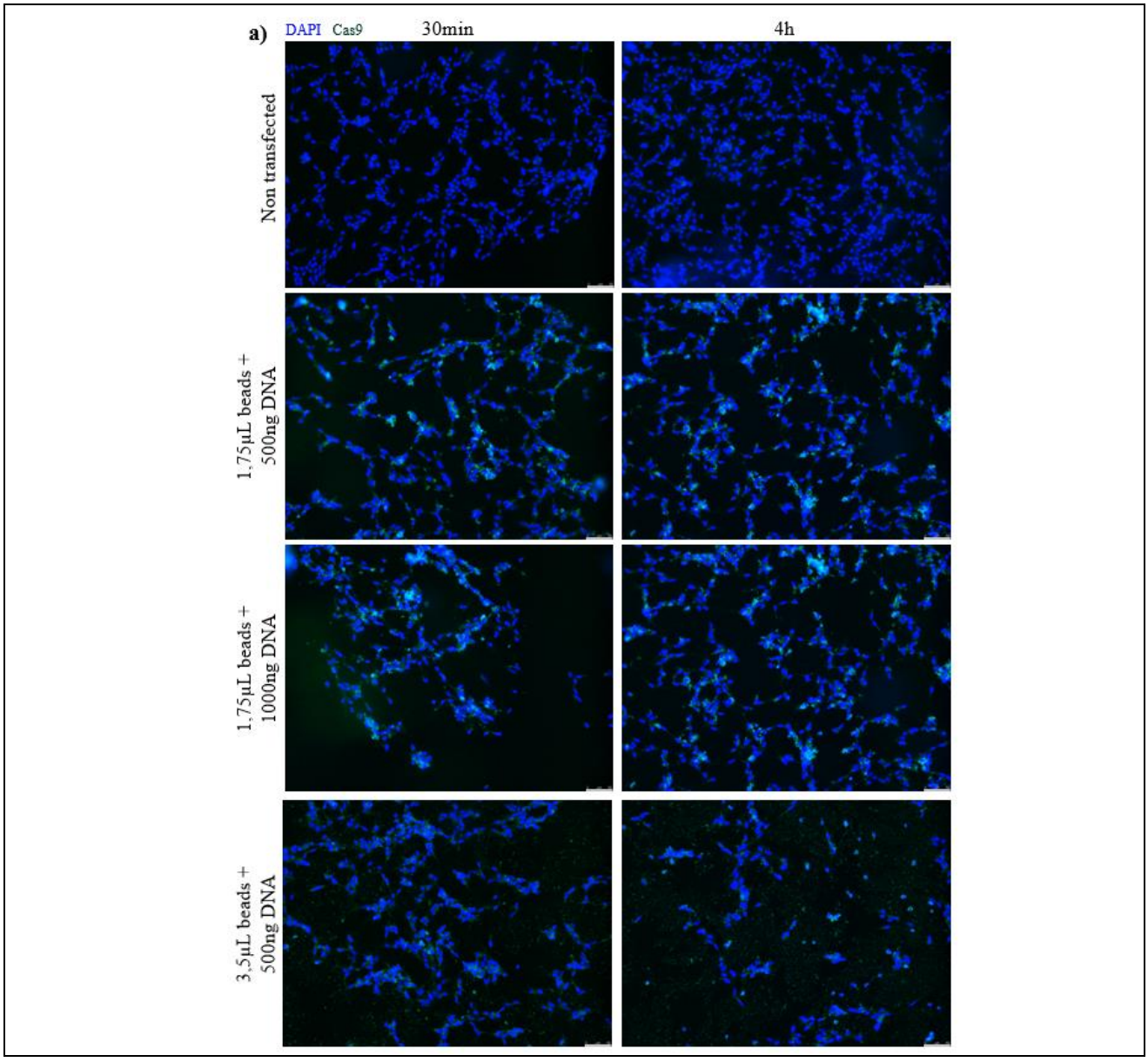

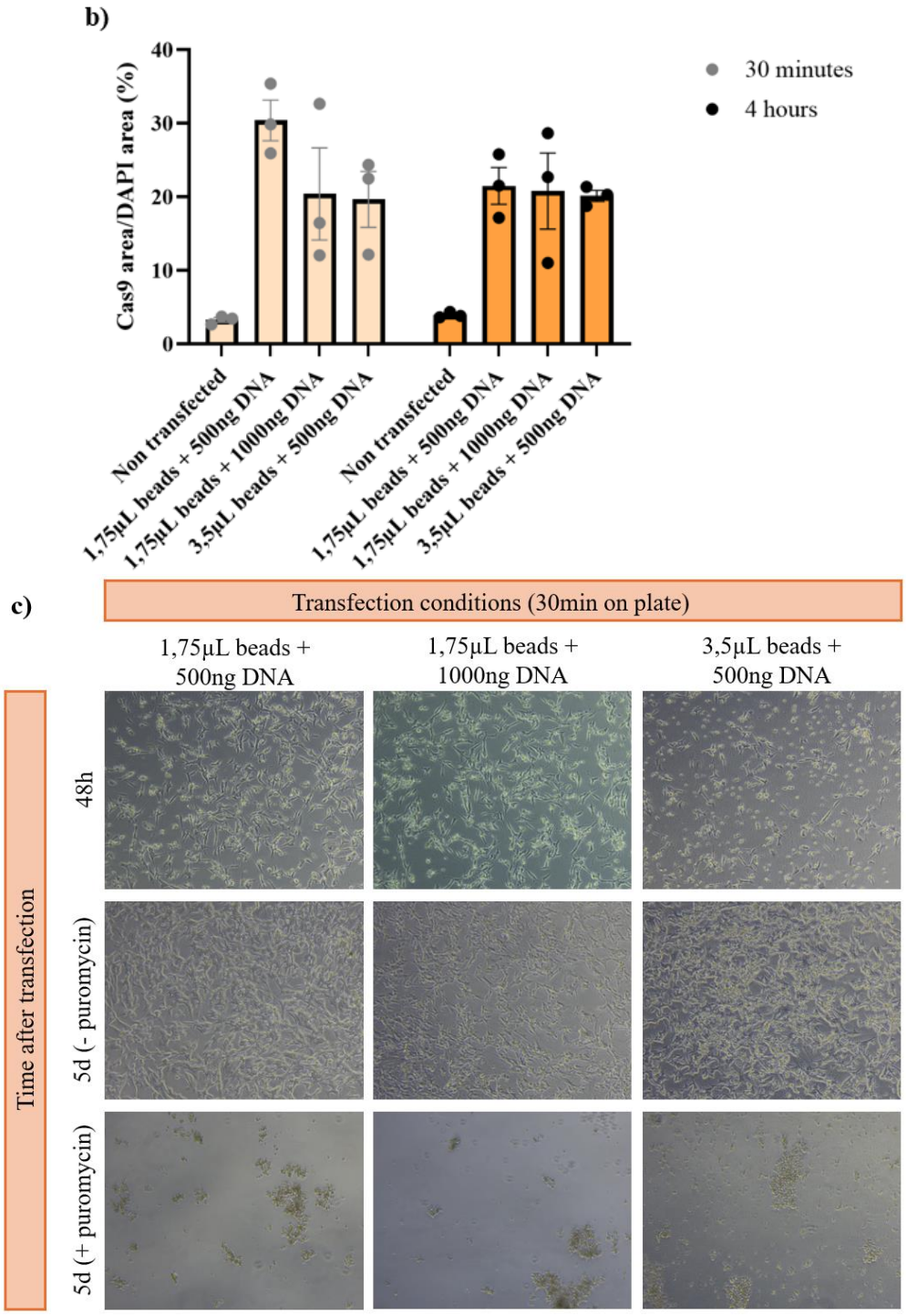

Figure 5 – Successfully transfected SH-SY5Y cells with PDE4Dpan plasmid DNA. (a) Immunocytochemistry stainings of the SH-SY5Y cell nuclei (DAPI, blue) and Cas9 (green). Six different conditions of transfection were tested, including 1,75µL or 3,5µL of magnetic beads, 500ng or 1000ng of plasmid DNA, and 30min or 4h on the magnetic plate. Non transfected SH-SY5Y cells were utilized as a negative control. The scale bar represents 50µm (20x magnification). **(b)** Quantification of the immunocytochemistry staining by dividing the Cas9 area present on the images by the DAPI area, expressed in percentage (%). **(c)** Light microscopy images at 20x magnification of the three transfection conditions with 30min on the magnetic plate after 48h of transfection and after 5d, with and without puromycin administration as a selection method. Data are represented as mean ± SEM (n = 1, three measurement points). *PDE4D; phosphodiesterase 4D, DAPI; 4',6-diamidino-2-phenylindole, Cas9; CRISPR associated protein 9, µL; microliter, ng; nanograms, µm; micrometer.*

DISCUSSION

Since memory loss is the primary symptom of AD and not all patients respond to the psychotropic medications used nowadays, it is important to unravel and comprehend the molecular processes and mechanisms involved in memory consolidation to develop more effective and personalized treatments for these patients (7-10). The PDE4 enzymes are inhibitors of the cAMP-PKA-CREB pathway of memory consolidation, which is why targeting these enzymes could improve memory loss in patients with AD (12-14, 20). As PDE4- and PDE4D inhibitors still cause side effects, a more selective approach focusing on the isoforms of the PDE4D subtype is interesting and more targeted (21-23). Therefore, this research focused on taking the first step in selectively ablating the PDE4D isoforms independently by CRISPR/Cas9 and investigating in the effect on a human neuronal cell line (SH-SY5Y cells) *in vitro*. Consequently, it was necessary to investigate the expression pattern of the PDE4D isoforms in SH-SY5Y cells before continuing with further experiments. It is necessary to mention that no primers could specifically detect the PDE4D2 isoform as this super short isoform of 507 amino acids long has only very little upstream conserved region 1 (UCR1) specific for this isoform. Therefore, the expression of PDE4D2 was not taken into account (Figure 1) (22). After 48h of cell culture (Figure 1a), the mRNAs of all isoforms were expressed, except for PDE4D7, even though this isoform is known to be expressed in the brain (12, 28). Recent research does validate the expression of PDE4D7 in mouse neuroblastoma cell lines (e.g. N2a cells) and mouse hippocampal cell lines (e.g. HT22 cells), but not yet in human neuroblastoma/hippocampal cell lines (25). Therefore, it is interesting to further investigate in which human cell line this isoform is expressed, such as the Neu41 cell line (human neuron progenitor cell line) or human iPSCs-derived cortical neurons. However, PDE4D7 was shown to have a very high mRNA expression in the area postrema – the chemoreceptor trigger zone for emesis in the brain stem – of the human brain (29). Therefore, it is a less interesting target for ablation, as this could enhance the adverse side effects, an aspect we intend to prevent. Finally, after 96h of cell culture, an adequate expression of PDE4D isoforms in SH-SY5Y cells was detected by qPCR, indicating that time is not a determining variable in the case of PDE4D isoform expression.

Another aspect of this study is the investigation of the PDE4D isoform expression of SH-SY5Y cells in comparison to SH-SY5Y cells treated with $A\beta_{1-42}$. In doing so, we could detect the potential difference in PDE4D expression in a normal and AD-like model *in vitro*. No significant differences between the two groups were observed, although there was a clear increasing trend for PDE4D6 after $A\beta_{1-42}$ treatment (Figure 2). Our team has previously investigated the increased expression levels of PDE4D isoforms in the middle temporal gyrus tissue of AD patients and found that the mRNA expression of PDE4D1, -3, -5, and -8 were significantly increased (12). These data do not correspond to our qPCR data of the SH-SY5Y cells with/without $A\beta_{1-42}$ exposure, except for PDE4D8. For this isoform, only a small trend (p-value = 0.1429) was visible (Figure 2). These various outcomes can be explained by the difference between a human neuroblastoma cell line and the human brain of an AD patient. Conventional cell lines such as SH-SY5Y cells are readily available, but their implementation requires immortalized or malignant cells that are cultivated for several generations. This can result in differences in their physiological and genetic characteristics and, therefore, do not represent the primary tissue cell exquisitely (30, 31). On the contrary, the human post-mortem brain is much more complex, as it is a heterogeneous mix of cell types, such as neurons, glial cells, and astrocytes, that interact with each other. However, since Paes *et al.* utilized homogenized brain tissue, follow-up studies investigating whether the interaction of different cell types and PDE4D isoform expression and activity is essential in AD are still necessary (12). Furthermore, Y.Y. Sin *et al.* provided evidence that $A\beta_{1-42}$ can directly bind to PDE4D in a region at the start of the catalytic core, which will activate the long isoform PDE4D5. As now both upregulated mRNA expression and increased activity of the long PDE4D5 isoform in AD models are shown, this isoform can be a key target in this disease (12, 32). Although both papers conclude that PDE4D5 is influenced by $A\beta_{1-42}$, this is likely dependent on $A\beta_{1-42}$ dosing (Figure 2). Therefore, testing different concentrations of $A\beta_{1-42}$ on SH-SY5Y cells and increasing the sample size are future enhancements to validate our data. Nevertheless, the data of our study indicate that the levels of PDE4D isoforms are trend-like increasing in an AD-like model *in vitro*.

As the ultimate goal of this project is to ablate the different PDE4D isoforms independently, CRISPR/Cas9 plasmids for each isoform were designed by Benchling.com and developed with the PX459 vector (Supplementary Table 1). The design and development were successful for every PDE4D isoform, except for PDE4D2, due to the very little upstream UCR1 region of this isoform as already explained before. Furthermore, a pan sgRNA was designed to ablate the whole PDE4D subtype. To validate the efficacy of the designed sgRNAs on the DNA of SH-SY5Y cells, an *in vitro* cleavage assay was performed. Other validation steps could be a qPCR analysis or Western Blot. However, the primers of the PDE4D isoforms for qPCR analyses also detect a cleaved or unfunctional PDE4D gene, as these disruptive mutations are created at those cleavage sites by error-prone repair or by using homologous recombination to change or insert sequences (33). Therefore, qPCR is not an accurate method to validate the lower expression of PDE4D isoforms. In addition, a Western Blot analysis is not usable for these protein isoforms, as there are currently no specific and functional antibodies for each isoform independently. This highlights the relevance of the *in vitro* cleavage assay, as this assay indicates the efficacy of the sgRNAs designed for the PDE4D isoforms. In this paper, we successfully demonstrated that the sgRNAs designed for the isoforms PDE4D3, -5, -9, and -pan cleaved the amplicon of the DNA of the SH-SY5Y cells as expected (Figure 3, Supplementary Table 3). As a future perspective, Sanger sequencing can be applied to further validate the efficiency of the sgRNAs after transfection into the SH-SY5Y cells. Although Sanger sequencing used to have trouble with resolving small indels, there is currently an algorithm named the Tracking of Indels by Decomposition (TIDE), specified for detecting these indels (34).

Next to the sgRNA design and development, the transfection protocol by magnetofection needed to be optimized for the human neuron cell line based on previous work (25, 35). According to the protocol of the NeuroMag transfection reagent of Oz Biosciences, different conditions were included for magnetofection, including 1,75µL or 3,5µL of magnetic beads, 500ng or 1000ng of plasmid DNA, and 30min or 4h on the magnetic plate. This was verified by the quantification of the immunocytochemistry images (Figure 5a), in which was apparent that the condition of 1,75µL of magnetic beads, 500ng of plasmid DNA, and 30min on the magnet was the most optimal for transfection in SH-SY5Y cells, represented as 30% of Cas9/DAPI area compared to the other conditions with approximately 20% Cas9/DAPI area. The higher the Cas9/DAPI area, the more transfection was successful. In addition, as visible on the immunocytochemistry staining images of 3,5µL beads with 500ng DNA condition (Figure 4a), there are additional Cas9 spots in the background. This debris can cause a disturbed environment for the cells, and therefore be less effective for transfection. Consequently, we did not test the condition of 3,5µL magnetic beads and 1000ng plasmid DNA. Although a 30% Cas9/DAPI area is a good start for transfection efficiency, research by Paes *et al*. indicated that a transfection efficiency of 50% is feasible in the HT22 mouse hippocampal cell line (36). However, they checked for transfection efficiency after 48h, while we checked for 5d after transfection (36). Therefore, cells keep multiplying, causing the overall percentage of Cas9/DAPI area to decrease. To further improve transfection efficiency, the time of the transfected cells on the magnet can still be optimized, as 30min and 4h are still different from each other. Knowing 30min for the condition with 1,75µL of beads and 500ng of plasmid DNA has a higher percentage of Cas9/DAPI area than 4h, periods such as 45 minutes or 1 hour can be optional. In addition, the medium of the transfected cells was changed to medium with puromycin 48h after transfection, while this could be extended to 72h according to previous research of our team (35). This could lead to a longer exposure of the magnetic beads with plasmid DNA to the cells, possibly increasing the transfection efficiency. As the transfection protocol of NeuroMag is straightforward, other options to optimize the transfection could be focused on the cells, such as a lower passage number (now passage 31), or the density of the cells can be adjusted.

After successful transfection of the SH-SY5Y cells, it is important to select the transfected cells for further experiments focused on for example neurite outgrowth. The PX459 vector has a puromycin selection marker, which is why this antibiotic was chosen as the selection reagent for the transfected SH-SY5Y cells. Our team already utilized puromycin as a selection reagent in various cell types (37-39). However, as already explained before, this was not yet optimized in SH-SY5Y cells. Therefore, an MTT assay to determine the number of viable cells and

immunocytochemistry staining for the cell nuclei with DAPI were performed (Figure 4a, b). A dose-optimized concentration of puromycin is defined as the lowest concentration with 100% mortality in non-transfected cells (38). According to this definition and our data, 1µg/mL puromycin is the optimal concentration for SH-SY5Y cells. In addition, research by Hashemabadi *et al*. stated that they administered 1µg/mL as well to transfected SH-SY5Y cells with the PX459 plasmid (27). Unfortunately, all cells died after 72h of puromycin administration (Figure 5c). Therefore, we can conclude that 1µg/mL is a lethal concentration for transfected SH-SY5Y cells. A possible explanation for this cell death might be because the SH-SY5Y cells in the Hashemabadi *et al*. publication were exposed to 1µg/mL puromycin for 48h instead of 72h, causing a higher exposure to the cells in our study and possible lethality. However, after 48h of puromycin administration, we already saw the lethal effect on the cells. Furthermore, the MTT data shows that 0,5µg/mL is also no optimal concentration to utilize, as more than 50% of the SH-SY5Y cells survive and are metabolically active (Figure 4a). Therefore, a further investigation in the concentrations between 0,5 and 1µg/mL is necessary to optimize the puromycin concentration, like for example 0,75µg/mL. This is the last stage of the optimization process of the magnetofection of the PDE4Dpan sgRNA into the nuclei of the SH-SY5Y cells. This is a foundation for further experiments regarding the effects of ablating the PDE4D isoforms independently on neurite outgrowth and neuronal functioning in an AD context.

FUTURE PERSPECTIVES

This study provides a near-optimized protocol for the transfection by magnetofection of the PDE4D sgRNAs into the nuclei of the SH-SY5Y cells. In addition, this study shows that there is a trend in the upregulation of PDE4D isoforms in SH-SY5Y cells after exposure to $A\beta_{1-42}$ for 24h, in particular the upregulation of the PDE4D6 isoform. This, together with earlier findings of upregulation of PDE4D1, -3, -5, and -8 in AD post-mortem brains of patients with cognitive problems and its correlation with Aβ plaque load, confirms that these isoforms can be potential targets in this disease (12). However, this research did not investigate the effect of the ablation of the specific PDE4D isoforms in a normal and AD context, which would be the next logical step in order to unravel the molecular processes behind the different isoforms of the enzyme family in memory consolidation. To start, the efficacy of the other sgRNAs designed for the human PDE4D isoforms can be validated by the *in vitro* transcription assay, as performed for four sgRNAs in this study (Figure 3). After this validation step, the sgRNAs can be transfected into the cells according to the near-optimized protocol based on this study. Further experiments can be focused on neurite outgrowth, as this is an important characteristic of structural neuroplasticity, possibly increasing the knowledge of the effects of the individual isoforms in AD. Therefore, techniques such as immunocytochemistry staining of biomarkers, qPCR, and Western Blot analysis to determine the expression of important genes and proteins respectively in neurite elongation (e.g. MAP2, BDNF, NGF, NT-3) can be utilized for this future perspective (40-42). However, we need to take into account that transcription of BDNF will be upregulated by phosphorylated CREB in case of higher cAMP levels (43). In addition, research on ibudilast, a PDE inhibitor, describes that after PDE inhibition and cAMP upregulation, several neurotrophic factors are upregulated, such as NT-3, NT-4, and NGF (44). Besides the immunocytochemistry staining, the IncuCyte can be utilized in combination with the NeuroTrack analysis, in which the neurite elongation can be measured (45). In addition, investigating the effects on the cAMP-PKA-CREB pathway after selective PDE4D isoform ablation can be a validation that the effects on neuroplasticity are a result of stimulating this pathway. To identify these effects, a qPCR and Western Bot analysis can be used to determine the relative expression of mRNA and proteins, respectively, of this cascade. In addition, the fluorescence resonance energy transfer (FRET) analysis is an interesting tool as it can visualize the PKA activity by detecting the energy transfer using fluorescent dyes on the molecules, which is essential in the cAMP-PKA-CREB pathway for memory consolidation as the activity of PKA causes phosphorylation of CREB, and this way executes its function in the pathway (46).

Besides investigating the effects of the individual PDE4D isoforms *in vitro*, it is interesting to validate these findings in AD *in vivo* models, such as the transgenic AD mice (APPswe/PS1dE9). In this mice model, the CRISPR/Cas9 designs can be administered via several delivery systems, such as the Adeno-

associated viruses (AAV), lentiviruses, or lipid nanoparticles. These delivery systems have their advantages, but also disadvantages, such as limited packing capacity, high costs, or inflammation. Nevertheless, they are already utilized in the clinical stage, confirming their therapeutic potential (47). Regarding cortical neurons, which are non-dividing cells, the AAV is the most potent delivery system as it can transfect both dividing and non-dividing cells. Furthermore, it is necessary to target these AAVs specifically to the cortical neurons in the brain, by for example targeting them to the neuronal marker NeuN (48). Besides, the optimal route of administration has to be determined, such as the intranasal, subcutaneous, or intravenous route. To validate that the CRISPR/Cas9 system has reached the neurons in the brain specifically, a GFP reporter can be incorporated and the green fluorescent color present in the cells can be investigated *ex vivo* (49). After optimizing the delivery strategy of the sgRNAs to the brain of the AD mice, the effect on neuroplasticity and memory can be examined. Therefore, behavioral tests such as the object location task (OLT), object recognition task (ORT), or Y-maze can be utilized, as they reflect the spatial memory of the mice (25). In addition, post-mortem analysis of the brain of the mice can be of added value as immunohistochemistry stainings of the hippocampus or cerebral cortex of the mice can visualize the neuroplasticity and the correlations with the outcomes on the behavioral tests.

Since the ultimate goal is to reduce memory loss in patients with AD, the translation to the clinical setting is of utmost importance. Therefore, human *in vitro* models can be already of added value, such as human iPSC-derived cortical neurons. They represent a more translational approach to the human setting in comparison to neuroblastoma cell lines or animal models (50). Bringing CRISPR/Cas9 eventually to human participants in clinical studies is possible, but still contains some ethical concerns (33). Therefore, designing specific inhibitors for the PDE4D isoforms can be an interesting approach for further investigations, both in preclinical and clinical settings. This personalized treatment can be more accessible for AD patients with memory loss, as they receive a very targeted therapy that could stimulate memory consolidation without causing side effects like nausea and vomiting.

CONCLUSION

Altogether, we got an insight into PDE4D isoform expression in these cells, with and without $A\beta_{1-42}$ exposure, highlighting PDE4D6 as a potential target. Furthermore, we defined a near-optimized protocol for the successful transfection of CRISPR/Cas9 sgRNAs into the nuclei of the human SH-SY5Y cells. This transfection protocol can be utilized for further experiments regarding determining the effect of ablating the different PDE4D isoforms on neurite elongation and memory consolidation in human neurons *in vitro*, but it can also further open doors for *in vivo* studies and clinical trials for AD patients suffering from memory loss.

REFERENCES

1. Chavan AB, Patil SR, Patel AM, Chaugule SV, Gharal SK. A Comprehensive Review on Alzheimer's Disease its Pathogenesis, Epidermiology, Diagnostics and Treatment. Journal for Research in Applied Sciences and Biotechnology. 2023;2(4):66-72.
2. Rahman MM, Lendel C. Extracellular protein components of amyloid plaques and their roles in Alzheimer's disease pathology. Molecular Neurodegeneration. 2021;16(1):1-30.
3. Kosel F, Pelley JM, Franklin TB. Behavioural and psychological symptoms of dementia in mouse models of Alzheimer's disease-related pathology. Neuroscience & Biobehavioral Reviews. 2020;112:634-47.
4. Padovani A, Falato S, Pegoraro V. Extemporaneous combination of donepezil and memantine to treat dementia in Alzheimer disease: evidence from Italian real-world data. Current Medical Research and Opinion. 2023;39(4):567-77.
5. Kent SA, Spires-Jones TL, Durrant CS. The physiological roles of tau and Abeta: implications for Alzheimer's disease pathology and therapeutics. Acta Neuropathol. 2020;140(4):417-47.
6. Thal DR, Tome SO. The central role of tau in Alzheimer's disease: From neurofibrillary tangle maturation to the induction of cell death. Brain Res Bull. 2022;190:204-17.
7. Scheltens P, De Strooper B, Kivipelto M, Holstege H, Chételat G, Teunissen CE, et al. Alzheimer's disease. The Lancet. 2021;397(10284):1577-90.
8. Kaushik M, Kaushik P, Parvez S. Memory related molecular signatures: The pivots for memory consolidation and Alzheimer's related memory decline. Ageing Research Reviews. 2022;76:101577.
9. Cummings J. Drug development for psychotropic, cognitive-enhancing, and disease-modifying treatments for alzheimer's disease. The Journal of neuropsychiatry and clinical neurosciences. 2021;33(1):3-13.
10. Balázs N, Bereczki D, Kovács T. Cholinesterase inhibitors and memantine for the treatment of Alzheimer and non-Alzheimer dementias. Ideggyogy Sz. 2021;74(11-12):379-87.
11. Atri A. The Alzheimer's Disease Clinical Spectrum: Diagnosis and Management. Med Clin North Am. 2019;103(2):263-93.
12. Paes D, Lardenoije R, Carollo RM, Roubroeks JAY, Schepers M, Coleman P, et al. Increased isoform-specific phosphodiesterase 4D expression is associated with pathology and cognitive impairment in Alzheimer's disease. Neurobiol Aging. 2021;97:56-64.
13. Chen Y, Huang X, Zhang YW, Rockenstein E, Bu G, Golde TE, et al. Alzheimer's beta-secretase (BACE1) regulates the cAMP/PKA/CREB pathway independently of beta-amyloid. J Neurosci. 2012;32(33):11390-5.
14. Amidfar M, de Oliveira J, Kucharska E, Budni J, Kim Y-K. The role of CREB and BDNF in neurobiology and treatment of Alzheimer's disease. Life sciences. 2020;257:118020.
15. Colucci-D'Amato L, Speranza L, Volpicelli F. Neurotrophic factor BDNF, physiological functions and therapeutic potential in depression, neurodegeneration and brain cancer. International journal of molecular sciences. 2020;21(20):7777.
16. She L, Tang H, Zeng Y, Li L, Xiong L, Sun J, et al. Ginsenoside RK3 promotes neurogenesis in Alzheimer's disease through activation of the CREB/BDNF pathway. Journal of Ethnopharmacology. 2024;321:117462.
17. Grochowska KM, Gomes GM, Raman R, Kaushik R, Sosulina L, Kaneko H, et al. Jacob-induced transcriptional inactivation of CREB promotes Aβ-induced synapse loss in Alzheimer's disease. The EMBO Journal. 2023;42(4):e112453.
18. Sanders O, Rajagopal L. Phosphodiesterase inhibitors for Alzheimer's disease: a systematic review of clinical trials and epidemiology with a mechanistic rationale. Journal of Alzheimer's Disease Reports. 2020;4(1):185-215.
19. Gong Y, Chen J, Jin Y, Wang C, Zheng M, He L. GW9508 ameliorates cognitive impairment via the cAMP-CREB and JNK pathways in APPswe/PS1dE9 mouse model of Alzheimer's disease. Neuropharmacology. 2020;164:107899.
20. Bhat A, Ray B, Mahalakshmi AM, Tuladhar S, Nandakumar D, Srinivasan M, et al. Phosphodiesterase-4 enzyme as a therapeutic target in neurological disorders. Pharmacological research. 2020;160:105078.

21. Vanmierlo T, Creemers P, Akkerman S, van Duinen M, Sambeth A, De Vry J, et al. The PDE4 inhibitor roflumilast improves memory in rodents at non-emetic doses. Behavioural Brain Research. 2016;303:26-33.
22. Paes D, Schepers M, Rombaut B, van den Hove D, Vanmierlo T, Prickaerts J. The Molecular Biology of Phosphodiesterase 4 Enzymes as Pharmacological Targets: An Interplay of Isoforms, Conformational States, and Inhibitors. Pharmacol Rev. 2021;73(3):1016-49.
23. Wei X, Yu G, Shen H, Luo Y, Shang T, Shen R, et al. Targeting phosphodiesterase 4 as a therapeutic strategy for cognitive improvement. Bioorganic Chemistry. 2023;130:106278.
24. Zhang C, Xu Y, Zhang HT, Gurney ME, O'Donnell JM. Comparison of the Pharmacological Profiles of Selective PDE4B and PDE4D Inhibitors in the Central Nervous System. Sci Rep. 2017;7:40115.
25. Paes D, Schepers M, Willems E, Rombaut B, Tiane A, Solomina Y, et al. Ablation of specific long PDE4D isoforms increases neurite elongation and conveys protection against amyloid-β pathology. Cellular and Molecular Life Sciences. 2023;80(7):178.
26. Chandrasekaran A, Toh KY, Low SH, Tay SKH, Brenner S, Goh DLM. Identification and characterization of novel mouse PDE4D isoforms: molecular cloning, subcellular distribution and detection of isoform-specific intracellular localization signals. Cellular signalling. 2008;20(1):139-53.
27. Hashemabadi M, Sasan H, Amandadi M, Esmaeilzadeh-Salestani K, Esmaeili-Mahani S, Ravan H. CRISPR/Cas9-mediated disruption of ZNF543 gene: an approach toward discovering its relation to TRIM28 gene in Parkinson's disease. Molecular Biotechnology. 2023;65(2):243-51.
28. Gurney ME. Genetic association of phosphodiesterases with human cognitive performance. Frontiers in molecular neuroscience. 2019;12:22.
29. Schepers M, Paes D, Tiane A, Rombaut B, Piccart E, van Veggel L, et al. Selective PDE4 subtype inhibition provides new opportunities to intervene in neuroinflammatory versus myelin damaging hallmarks of multiple sclerosis. Brain Behav Immun. 2023;109:1-22.
30. Kaur G, Dufour JM. Cell lines: Valuable tools or useless artifacts. Spermatogenesis. 2012;2(1):1-5.
31. Ranjan VD, Qiu L, Tan EK, Zeng L, Zhang Y. Modelling Alzheimer's disease: Insights from in vivo to in vitro three-dimensional culture platforms. Journal of tissue engineering and regenerative medicine. 2018;12(9):1944-58.
32. Sin YY, Cameron RT, Schepers M, MacLeod R, Wright TA, Paes D, et al. Beta-amyloid interacts with and activates the long-form phosphodiesterase PDE4D5 in neuronal cells to reduce cAMP availability. FEBS Lett. 2024.
33. Zheng R, Zhang L, Parvin R, Su L, Chi J, Shi K, et al. Progress and Perspective of CRISPR-Cas9 Technology in Translational Medicine. Advanced Science. 2023;10(25):2300195.
34. Sentmanat MF, Peters ST, Florian CP, Connelly JP, Pruett-Miller SM. A Survey of Validation Strategies for CRISPR-Cas9 Editing. Sci Rep. 2018;8(1):888.
35. Tiane A, Schepers M, Reijnders RA, van Veggel L, Chenine S, Rombaut B, et al. From methylation to myelination: epigenomic and transcriptomic profiling of chronic inactive demyelinated multiple sclerosis lesions. Acta neuropathologica. 2023:1-17.
36. Paes D, Schepers M, Willems E, Rombaut B, Tiane A, Solomina Y, et al. Ablation of specific long PDE4D isoforms increases neurite elongation and conveys protection against amyloid-beta pathology. Cell Mol Life Sci. 2023;80(7):178.
37. Wouters E, De Wit NM, Vanmol J, Van der Pol SM, van Het Hof B, Sommer D, et al. Liver X receptor alpha is important in maintaining blood-brain barrier function. Frontiers in immunology. 2019;10:1811.
38. Tiane A, Schepers M, Riemens R, Rombaut B, Vandormael P, Somers V, et al. DNA methylation regulates the expression of the negative transcriptional regulators ID2 and ID4 during OPC differentiation. Cellular and Molecular Life Sciences. 2021;78:6631-44.
39. Diouf D, Vitale MR, Zöller JEM, Pineau A-M, Klopocki E, Hamann C, et al. Generation of a ST3GAL3 null mutant induced pluripotent stem cell (iPSC) line (UKWMPi002-A-3) by CRISPR/Cas9 genome editing. Stem Cell Research. 2023;67:103038.
40. Sánchez C, Dıaz-Nido J, Avila J. Phosphorylation of microtubule-associated protein 2 (MAP2) and its relevance for the regulation of the neuronal cytoskeleton function. Progress in neurobiology. 2000;61(2):133-68.

41. Wlodarczyk L, Szelenberger R, Cichon N, Saluk-Bijak J, Bijak M, Miller E. Biomarkers of angiogenesis and neuroplasticity as promising clinical tools for stroke recovery evaluation. International journal of molecular sciences. 2021;22(8):3949.
42. Bothwell M. NGF, BDNF, NT3, and NT4. Handb Exp Pharmacol. 2014;220:3-15.
43. Mussen F, Broeckhoven JV, Hellings N, Schepers M, Vanmierlo T. Unleashing Spinal Cord Repair: The Role of cAMP-Specific PDE Inhibition in Attenuating Neuroinflammation and Boosting Regeneration after Traumatic Spinal Cord Injury. Int J Mol Sci. 2023;24(9).
44. Angelopoulou E, Pyrgelis E-S, Piperi C. Emerging potential of the phosphodiesterase (PDE) inhibitor ibudilast for neurodegenerative diseases: an update on preclinical and clinical evidence. Molecules. 2022;27(23):8448.
45. Koulousakis P, Willems E, Schepers M, Rombaut B, Prickaerts J, Vanmierlo T, van den Hove D. Exogenous oxytocin administration restores memory in female APP/PS1 mice. Journal of Alzheimer's Disease. 2023(Preprint):1-19.
46. Depry C, Zhang J. Using FRET-based reporters to visualize subcellular dynamics of protein kinase A activity. Methods Mol Biol. 2011;756:285-94.
47. Behr M, Zhou J, Xu B, Zhang H. In vivo delivery of CRISPR-Cas9 therapeutics: Progress and challenges. Acta Pharm Sin B. 2021;11(8):2150-71.
48. Hana S, Peterson M, McLaughlin H, Marshall E, Fabian AJ, McKissick O, et al. Highly efficient neuronal gene knockout in vivo by CRISPR-Cas9 via neonatal intracerebroventricular injection of AAV in mice. Gene therapy. 2021;28(10):646-58.
49. Ablain J, Durand EM, Yang S, Zhou Y, Zon LI. A CRISPR/Cas9 vector system for tissue-specific gene disruption in zebrafish. Dev Cell. 2015;32(6):756-64.
50. Penney J, Ralvenius WT, Tsai L-H. Modeling Alzheimer's disease with iPSC-derived brain cells. Molecular psychiatry. 2020;25(1):148-67.

Acknowledgments – First, I would like to sincerely thank EW for her daily guidance throughout my internship. She helped me develop a critical mindset, acquire various new techniques, and become an independent researcher. Furthermore, I would like to thank TV for the opportunity to execute my internship at team RICE, and also for the opportunity to apply for a fellowship at FWO. For the latter, I am sincerely grateful for the guidance, support, and feedback of Dr. Ir. Inez Wens, my co-promotor for this application. I am grateful for the additional activities during my internship, such as the opportunity to participate and even present my project at conferences like EURON PhD Days and MS Research Days. Next, I would like to thank the whole RICE team for their help and support during lab meetings and in the laboratory, especially Dr. Melissa Schepers, Femke Mussen, and Ben Rombaut. In addition, I would like to thank my co-students in this team: Zoë Donders, with whom I also collaborated in the lab, and Freddy Leenders, for mental support. Furthermore, I would like to thank my second examiner Prof. Dr. Bert Brône for the help and feedback during the progress meetings. Lastly, I greatly appreciate my friends and family for their continuous support during this internship.

Author contributions – TV and EW conceived and designed the research. JR performed experiments and data analysis under the supervision of EW. Dr. Melissa Schepers and Zoë Donders assisted with the sgRNA design and development. JR wrote the paper and EW carefully edited the manuscript.

Supplementary information

Table 1: Designed sgRNAs by Benchling.com. *The overhang is depicted in red.*

PDE4D isoform	sgRNA (5'-3') with overhang	sgRNA (3'-5') with overhang
1	CACCGTCCGCTAGCGAGTTCAAAG	CAGGCGATCGCTCAAGTTTCCAAA
3	CACCGATATCCAGGAATGCCTTCTAAA	CTATAGGTCCTTACGGAAGATTTCAAA
4	CACCGGACCGCACCTCCTACGCGG	CCTGGCGTGGAGGATGCGCCCAAA
5	CACCGCAAACAGCGGCGTTTCACGG	CGTTTGTCGCCGCAAAGTGCCCAAA
6	CACCGAAACTATTTACTGTCAGTGTCTTG	CTTTGATAAATGACAGTCACAGAACCAAA
7	CACCGTAGGGTTCCATTCCGCGGAA	CATCCCAAGGTAAGGCGCCTTCAAA
8	CACCGCTCTTGTAGATGGTCCTGGCACCG	CGAGAACATCTACCAGGACCGTGGCCAAA
9	CACCGCCCGATCTACAAGTTCCCTA	CGGGCTAGATGTTCAAGGGATCAAA
Pan	CACCGTGGACGGACCGGATAATGG	CACCTGCCTGGCCTATTACCCAAA

PDE4D; phosphodiesterase 4D, sgRNA; single guide RNA.

Table 2: PDE4D isoform qPCR primers (Integrated DNA Technologies).

PDE4D isoform	Forward primer	Reverse primer
1	5'-AGAACTGAGTCCCCCTTTCC-3'	5'-TGAGCTCCCGATTAAGCATC-3'
3	5'-CCACGATAGCTGCTCAAACA-3'	5'-GTGCCATTGTCCACATCAAAA-3'
4	5'-TCTGGCGCCTTCAAGTGAGA-3'	5'-CAGAGATGCTTGGGGGCTTT-3'
5	5'-TGTTGCAGCATGAGAAGTCC-3'	5'-ATGTATGTGCCACCGTGAAA-3'
6	5'-ATTCGATGGGAAGACGGCTG-3'	5'-CCACAAGCCACGCAGAGTAT-3'
7	5'-GAACATTCAACGACCAACCA-3'	5'-TTCCGGGACATCATAGACTTTGG-3'
8	5'-CGCACCAGCTCTGACTTCTC-3'	5'-CGCAATCTTGATTTGGCTCT-3'
9	5'-ATGCTGGTTTCCCTTGTGAC-3'	5'-ATGGGCAAGGTTCTAACACG-3'

Table 3: Primers for SH-SY5Y genomic amplicon generation for the in vitro transcription.

PDE4D isoform	Forward primer (5'-3')	Reverse primer (3'-5')	Ampli-con size	Fragment sizes
1	CGCATAGTGGTTTTTCCGCT	GCTGCAAGGGCTCAGTGTTA	690	242+488
3	TAAATGGATGGACCCATACCTGC	GAAATTCATGTGTGCCCTTCCCC	671	274+397
4	GCGCCTTCAAGTGAGAAGCTA	AAGGATAGGCACACCCCTGT	758	525+233
5	CGTGGCTGAACGAAGACCT	CTCTGTCCAAGTGGGGATCAT	636	180+456
6	CACACCCCCTCGCCTTATAG	CCACATGACAAACAGAAGAACTAC	780	527+253
7	GTTTTAACCAAGCCACACCTGG	CACCAATACATTTTCAGCTCTTCCA	678	271+407
8	AACGAAGCCCTGTGGGTTTAC	AAAGGCTTATTTGCAAGGGGC	604	478+126
9	AAAGCGCTCCTGCGTGTTA	AAGACAAGGGCAAAGCCTGTC	629	236+393
Pan	ACATCATGGTTGAGCTGTTTGG	AGTTGTTGACATGGTAGGGCTTAT	663	233+430

Table 4: sgRNA 58bp forward templates for the in vitro transcription*. Extra sequence (4bp) in green, T7 promotor (17bp) in orange, extra G(s) added (0-2bp) in purple, target sequence (20-24bp) in black, and Scaffold Template annealing sequence (15bp) in blue.*

PDE4D isoform	Forward template
1	CCTCTAATACGACTCACTATAGGTCCGCTAGCGAGTTCAAAGGTTTAAGAGCTATGC
3	CCTCTAATACGACTCACTATAGGATATCCAGGAATGCCTTCTAAAGTTTAAGAGCTATGC

4	CCTCTAATACGACTCACTATAGGACCGCACCTCCTACGCGGGTTTAAGAGCTATGC
5	CCTCTAATACGACTCACTATAGGCAAACAGCGGCGTTTCACGGGTTTAAGAGCTATGC
6	CCTCTAATACGACTCACTATAGGAAACTATTTACTGTCAGTGTCTTGGTTTAAGAGCTATGC
7	CCTCTAATACGACTCACTATAGGTAGGGTTCCATTCCGCGGAAGTTTAAGAGCTATGC
8	CCTCTAATACGACTCACTATAGGCTCTTGTAGATGGTCCTGGCACCGGTTTAAGAGCTATGC
9	CCTCTAATACGACTCACTATAGGCCCGATCTACAAGTTCCCTAGTTTAAGAGCTATGC
Pan	CCTCTAATACGACTCACTATAGGTGGACGGACCGGATAATGGGTTTAAGAGCTATGC

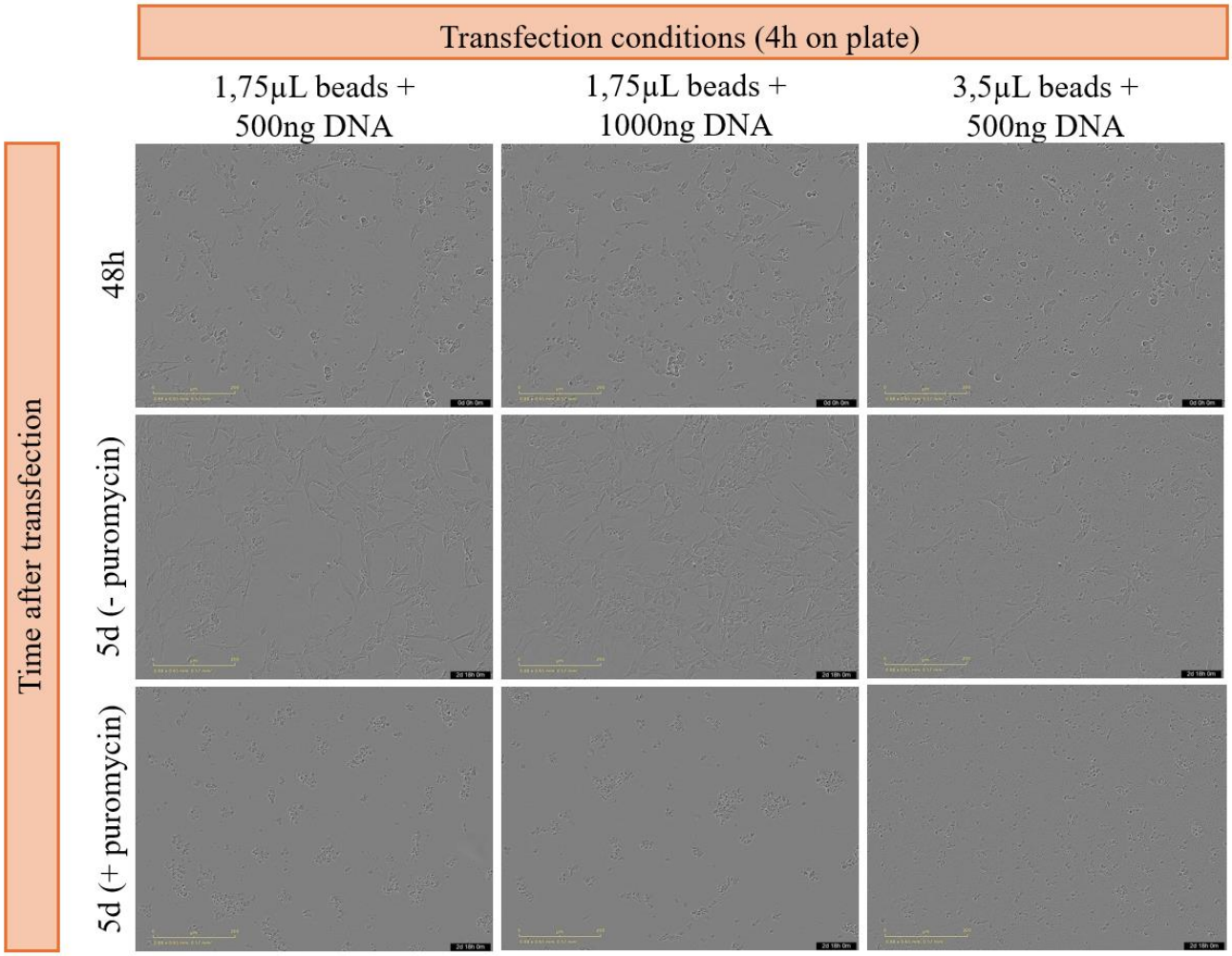

Figure S1 – Puromycin administration to the SH-SY5Y cells after transfection with different conditions (4h on the magnetic plate). IncuCyte images at 20x magnification of the three transfection conditions with 4h on the magnetic plate after 48h of transfection and 5d, with and without 1µg/mL puromycin administration. The scale bar represents 200µm. *h; hours, d; days, µL; microliter, ng; nanograms, µm; micrometer.*